Inorganica Chimica Acta 571 (2024) 122203

Contents lists available at ScienceDirect

Inorganica Chimica Acta

journal homepage: www.elsevier.com/locate/ica

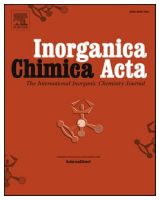

Research paper

Anion- and water-facilitated oxidative carbon–carbon bond cleavage and diketonate carboxylation in Cu(II) chlorodiketonate complexes

Josiah G.D. Elsberg [a], Tomasz Borowski [b], Eric W. Reinheimer [c], Lisa M. Berreau [a,*]

[a] Department of Chemistry and Biochemistry, Utah State University, 0300 Old Main Hill, Logan, UT 84322-0300, USA
[b] Jerzy Haber Institute of Catalysis and Surface Chemistry, Polish Academy of Sciences, Krakow 30-239, Poland
[c] Rigaku Americas Corporation, 9009 New Trails Drive, The Woodlands, TX 77381, USA

ARTICLE INFO

Keywords:
Copper
Oxygen activation
Ligand
Mechanism
Hydrogen bonding

ABSTRACT

The O_2-dependent carbon–carbon (C—C) bond cleavage reactions of the mononuclear Cu(II) chlorodiketonate complexes [(6-Ph_2TPA)Cu(PhC(O)CClC(O)Ph)]ClO_4 (**1-ClO$_4$**) and [(bpy)Cu(PhC(O)CClC(O)Ph)(ClO_4)] (**3-ClO$_4$**) have been further examined in terms of their anion and water dependence. The bpy-ligated Cu(II) chlorodiketonate complex **3-ClO$_4$** is inherently more reactive with O_2 than the 6-Ph_2TPA-ligated analog **1-ClO$_4$**. Added chloride is needed to facilitate O_2 reactivity for **1-ClO$_4$** but not for **3-ClO$_4$** at 25(1) °C. Evaluation of k_{obs} for the reaction of **1-ClO$_4$** with O_2 under pseudo first-order conditions as a function of the amount of added chloride ion produced saturation type behavior. The bpy-ligated **3-ClO$_4$** exhibits different behavior, with rate enhancement resulting from both the addition of chloride ion and water. Computational studies indicate that the presence of water lowers the barrier for O_2 activation for **3-ClO$_4$** by ~12 kcal/mol whereas changing the anion from perchlorate to chloride has a smaller effect (lowering of the barrier by ~3 kcal/mol). Notably, the effect of water for **3-ClO$_4$** is of similar magnitude to the barrier-lowering chloride effect found in the O_2 activation pathway for **1-ClO$_4$**. Thus, both systems involve lower energy O_2 activation pathways available, albeit resulting from different ligand effects. Probing the effect of added benzoate anion, it was found that the chloro substituent in the diketonate moiety of **1-ClO$_4$** and **3-ClO$_4$** will undergo displacement upon treatment of each complex with tetrabutyl ammonium benzoate to give Cu(II) benzoyloxydiketonate complexes (**4** and **5**). Complexes **4** and **5** exhibit slow O_2-dependent C—C cleavage in the presence of added chloride ion. These results are discussed in the context of the chemistry identified for various divalent metal chlorodiketonate complexes, which have relevance to catalytic systems and metalloenzymes that mediate O_2-dependent C—C cleavage within diketonate substrates.

1. Introduction

Oxidative carbon–carbon (C—C) bond cleavage reactions facilitated by copper catalysts and involving O_2 as the terminal oxidant are of current interest for synthetic applications, including for reactions involving β-diketone substrates [1–5]. However, the reaction pathways by which cleavage processes of this type occur have not been extensively investigated [5–14]. It is noteworthy that little is currently known regarding how anions or water associated with the copper catalyst may influence O_2 activation reactivity. While some research has been done to explore the effects of halides on transition metal catalysis, only recently has there been examination of anion effects in copper-containing systems [15–18]. Other factors that influence O_2 activation, such as hydrogen bonding, also remain of current interest [19]. O_2-dependent C—C cleavage involving diketonate substrates is also important as such reactivity is relevant to the reaction catalyzed by diketone dioxygenase (Dke1) enzymes [20].

We have previously reported studies of the effect of added chloride anion on the O_2-dependent C—C bond cleavage reaction of the chlorodiketonate ligand in [(6-Ph_2TPA)Cu(PhC(O)CClC(O)Ph)]ClO_4 (**1-ClO$_4$**) (6-Ph_2TPA = *N,N*-bis((6-phenyl-2-pyridyl)methyl)-*N*-((2-pyridyl)methyl)amine [21,22]. When exposed to O_2, **1-ClO$_4$** undergoes reaction to form a Cu(II) chloride complex (**2**, Scheme 1(a)) and organic products resulting from C—C cleavage, including benzoic acid, benzil, benzoic anhydride, diphenylpropanetrione, and a CO_2/CO (0:80:0.05 eq) mixture. Strong evidence supports the involvement of diphenylpropanetrione as an intermediate in this reaction prior to C—C bond cleavage [22]. In our prior work, monitoring of the π-π* chlorodiketonate band in

* Corresponding author.
E-mail address: lisa.berreau@usu.edu (L.M. Berreau).

https://doi.org/10.1016/j.ica.2024.122203
Received 10 January 2024; Received in revised form 8 June 2024; Accepted 11 June 2024
Available online 19 June 2024

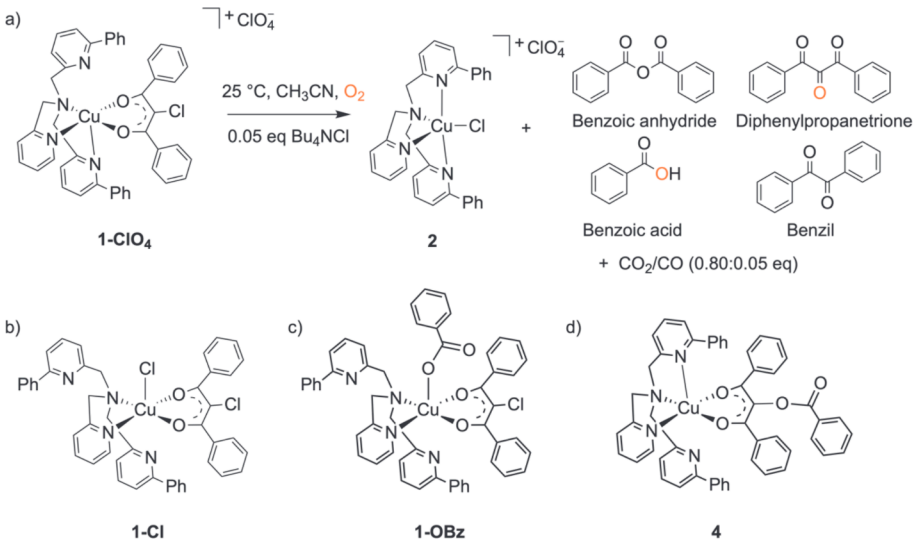

Scheme 1. a) O_2-dependent C—C bond cleavage reactivity of **1-ClO$_4$**. b) Proposed structure of chloro-adduct **1-Cl**. c) Proposed Cu-benzoato adduct **1-OBz**. d) Cu(II) benzoyloxydiketonato complex **4**.

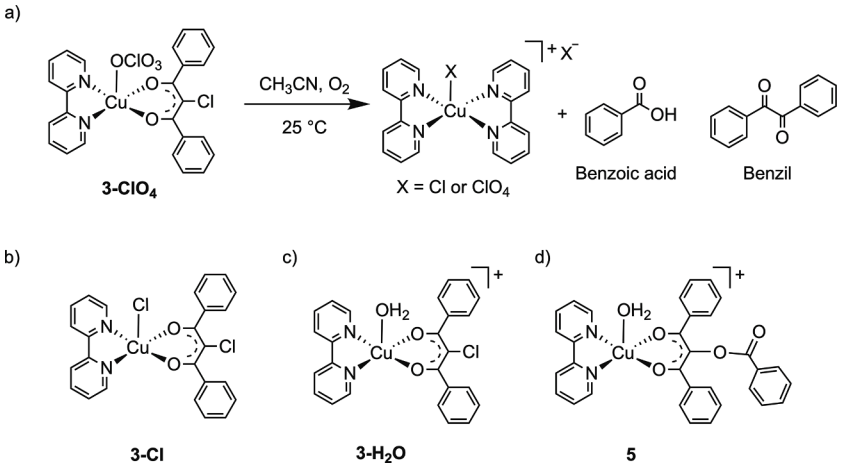

Scheme 2. a) O_2-dependent aliphatic C—C bond cleavage reactivity of **3-ClO$_4$**. b) Proposed structure of chloride-adduct **3-Cl**. c) Proposed H_2O adduct **3-H$_2$O**. d) Cu (II) benzoyloxydiketonato complex.

the reaction of **1-ClO$_4$** with O_2 under pseudo-first order conditions revealed a slow induction phase followed by a rapid first-order decay process. Notably, addition of a catalytic amount of chloride anion removed the induction phase, providing evidence for a lowering of the activation barrier for reaction with O_2. Computational studies of this process provided evidence that chloride coordination to the Cu(II) center lowered the barrier for O_2 activation by ~9 kcal/mol (from ~26 to 17 kcal/mol) [22]. Evidence from chloride binding studies with **1-ClO$_4$** suggested the formation of an adduct (**1-Cl**, Scheme 1(b)) with a binding constant of log K = 1.84(3) and Rose-Drago plots implying a two-state equilibrium involving **1-ClO$_4$** and **1-Cl** in the system. Use of $^{18}O_2$ in the reaction provided evidence for the incorporation of labeled oxygen atoms in the organic products [21].

As shown in Scheme 1(b) the optimized geometry of **1-Cl** from DFT calculations is suggested to have a square-pyramidal Cu(II) center with only the tertiary nitrogen and unsubstituted pyridyl donor from the 6-Ph$_2$TPA chelate ligand coordinating to the Cu(II) center. To evaluate the effect of a bidentate nitrogen donor supporting chelate ligand, a 2,2′-bipyridine (bpy)-ligated Cu(II) chlorodiketonate complex (**3-ClO$_4$**, Scheme 2(a)) was synthesized and found to have a similar square-pyramidal geometry via X-ray crystallography, with a perchlorate anion coordinated in the axial position [22]. In the presence of O_2, **3-ClO$_4$** exhibited the same type of oxidative cleavage reactivity as **1-ClO$_4$** (Scheme 2(a)), including an induction phase followed by a first-order decay. Like **1**, addition of chloride anion (via introduction of CH_3CN aliquots of [Bu$_4$N]Cl) to CH_3CN solutions of **3-ClO$_4$** resulted in the loss of the induction phase indicating a lowering of the barrier for O_2 activation. Chloride binding studies again provided evidence for a two-state equilibrium involving a possible chloride adduct (log K = 4.1(7); **3-Cl**, Scheme 2(b)). The larger log K value versus that found for **1-Cl** implies a stronger binding affinity for the anion in **3-Cl**.

Benzoate/benzoic acid is generated in the O_2-dependent C—C bond cleavage reaction of the chlorodiketonate ligand in **1-ClO$_4$** and **3-ClO$_4$**. To explore potential effects of the benzoate anion in the reaction, Saraf, *et al.* also examined the effect of added benzoate anion on the O_2 reactivity of **1-ClO$_4$** and **3-ClO$_4$** [22]. Interestingly, monitoring the π-π* diketonate absorption feature of each complex as a function of time indicated a longer induction phase versus the reaction having no added anion. In fact, in the case of **1**, increasing the amount of benzoate produced increasingly long induction phases. Axial benzoate coordination to the Cu(II) center similar to chloride in **1-Cl**, with log K = 2.81(2) for **1-OBz** (Scheme 1(c)) was proposed based on anion binding studies and

DFT calculations [22]. The computational studies suggested that benzoato coordination to **1** should lower the O_2 activation barrier similar to that of chloride. With this being the case, the difference in the respective effects of added chloride and benzoate anions on the induction phase remained to be fully understood. It is noteworthy that addition of chloride anion can "rescue" the benzoate-containing reaction for **1**, suggesting that the chloride-containing reaction provides the overall lowest energy pathway for O_2-dependent C—C cleavage [22].

The new results reported herein describe recent discoveries that we have made regarding the O_2 reactivity of **1-ClO$_4$.** Specifically, we have found that the previously reported chloride dependent reactivity of **1-ClO$_4$** depends on how the complex is isolated [21,22]. In the current work we show that **1-ClO$_4$** produced following multiple recrystallizations is *unreactive* with O_2 in absence of added chloride ion. This indicates that prior isolated precipitates of **1-ClO$_4$** that were used in the studies reported in references 22 and 23, which showed O_2 reactivity following an initial lag phase, likely contained chloride contaminants that may have resulted from *retro*-Claisen decomposition of the chlorodiketonate ligand [23]. Additionally, we further examined the products generated in reactions of **1-ClO$_4$** and **3-ClO$_4$** with Bu_4NOBz under O_2 [22]. We previously reported that addition of benzoate resulted in the formation of adducts (**1-OBz** and **3-OBz**) that lowered the barrier for reaction with O_2. New ESI-MS studies now provide evidence for competing benzoate substitution reactivity involving the chlorodiketonate ligand to produce Cu(II) benzoyloxydiketonate species (**4** and **5**) under O_2. This substitution reactivity is more prevalent for **3-ClO$_4$** than **1-ClO$_4$** under O_2, likely due to steric differences around the Cu(II) center. Under N_2, both **1-ClO$_4$** and **3-ClO$_4$** undergo substitution of the diketonate chloride substituent when treated with Bu_4NOBz to give **4** and **5**. The 6-Ph_2TPA-ligated Cu(II) benzoyloxydiketonate complex (**4**, Scheme 1) is stable with respect to O_2 whereas the bpy-ligated analog **5** shows slow O_2-dependent C—C cleavage in the presence of added chloride ion. Overall, the studies presented herein provide further insight into the novel anion-induced reactivity of **1-ClO$_4$** and **3-ClO$_4$** with O_2. Studies of the reactivity of these complexes are relevant toward understanding how anions and other molecules (e.g., water) can play a crucial role in Cu(II)-mediated oxidative processes involving O_2 activation.

2. Experimental

2.1. General methods

All solvents and reagents were purchased from commercial sources and were used without prior purification unless otherwise indicated. Solvents were dried following a previously published procedure and distilled prior to use [24]. *N,N*-bis((6-phenyl-2-pyridyl)methyl)-*N*-((2-pyridyl)methyl)amine (6-Ph_2TPA) and 2-chloro-1,3-diphenyl-1,3-propanedione were prepared according to literature procedures [25,26]. All manipulations involving the preparation and handling of the Cu(II) complexes were performed in an MBraun Unilab glovebox under an N_2 atmosphere unless otherwise indicated. Complex **3-ClO$_4$** was prepared and isolated as previously reported [22].

2.2. Physical methods

^1H and $^{13}C\{^1H\}$ NMR spectra were collected using a Bruker Advance III HD Ascend-500 spectrometer. Chemical shifts (ppm) are reported relative to the residual solvent peak in CD_3CN (^1H NMR: 1.94 ppm, quintet) or $CDCl_3$ (^1H NMR: 7.26 ppm, singlet). FTIR spectra were collected as dilute KBr (oven dried) pellets using a Shimadzu FTIR-8400 spectrometer. UV–vis data were collected on either a Hewlett-Packard 8453A diode array spectrometer or Cary 50 spectrometer. ESI mass spectral data were collected using a Shimadzu LCMS-2020. Elemental analyses were performed by Robertson Microlit Laboratories (Ledgewood, N.J.) or Atlantic Microlab (Norcross, GA).

Caution! Perchlorate compounds containing organic ligands are potentially explosive. These materials should be handled with care and in small quantities [27].

2.3. Updated synthesis and isolation procedure for 1-ClO$_4$ incorporating multiple recrystallizations

Under an inert atmosphere at ~30 °C, $Cu(ClO_4)_2{\cdot}6H_2O$ (0.135 mmol) was dissolved in CH_3CN (~3 mL) and the solution was added to solid 6-Ph_2TPA (0.135 mmol). The resulting deep blue solution was stirred for 30 min. In a separate container, 2-chloro-1,3-diphenyl-1,3-propanedione (0.135 mmol) was dissolved in Et_2O and added to solid lithium bis(trimethylsilyl)amide (0.135 mmol), becoming a turbid yellow solution that was stirred for five minutes. The two solutions were then combined and stirred for a minimum of two hours, resulting in the formation of a clear green solution. The solvent was removed under reduced pressure and the residual solid was then dissolved in CH_2Cl_2. A precipitate that remained was removed by passing the solution through a Celite plug. The filtrate was reduced to ~1 mL under reduced pressure. Green needle crystals were grown by diffusion of Et_2O into the filtrate. After isolation, the crystals were recrystallized a second time from CH_2Cl_2/Et_2O (52 mg, 45 %). Anal calc. for $C_{45}H_{36}CuN_4O_6Cl_2{\cdot}0.1CH_2Cl_2$: C, 62.14; H, 4.19; N, 6.43. Found: C, 61.76; H, 4.31; 6.45. Full characterization data for **1-ClO$_4$** (UV–vis, FTIR, mass spectrometry, EPR, X-ray crystallography) has been previously reported [21].

2.4. Kinetic studies of the O_2 reactivity of 1-ClO$_4$ and 3-ClO$_4$

A CH_3CN stock solution of **1-ClO$_4$** or **3-ClO$_4$** was made in an inert-atmosphere glovebox. An aliquot from this solution was added to a 1 mm quartz cuvette having a long neck and a Teflon stopcock. After closing the stopcock, the cuvette was taken out of the glovebox and filled to a total volume of ~600 μL with O_2-purged CH_3CN. After mixing, the headspace of the cell was twice purged with O_2 for 30 s, flipping the sealed cuvette a few times after each purge. To introduce chloride anion to the solution, an aliquot from a stock solution of tetrabutylammonium chloride in CH_3CN was added and the solution was mixed by flipping the sealed cuvette over 2–3 times. Each reaction mixture was monitored by UV–vis (π-π* band for chlorodiketonate ligand of **1-ClO$_4$** and **3-ClO$_4$**) as a function of time at ~25 °C. The amount of chloride anion added was 0.25, 0.50, 1.00 or 2.00 equivalents. Experiments involving tetrabutylammonium benzoate were performed in a similar manner.

2.5. Oxidative C—C cleavage product isolation and identification

A CH_3CN solution of **1-ClO$_4$** or **3-ClO$_4$** was made in air at a concentration of $1.75x10^{-3}$ M. Each solution was then purged with O_2 for one minute. A specific amount of tetrabutylammonium chloride was then added from a stock solution in CH_3CN. Experiments were performed under the following conditions to complement prior studies: (a) **1-ClO$_4$** + 2 eq Bu_4NCl under O_2; (b) **3-ClO$_4$** + 0–2 eq Bu_4NCl; (c) **1-ClO$_4$** + 0–2 eq Bu_4NOBz under O_2 or N_2; (d) **3-ClO$_4$** + 0–2 eq Bu_4NOBz under O_2 or N_2. Each sample was subsequently stirred for 16 h. Experiments containing Bu_4NCl changed from green to turbid light blue within 10 min. The mixture containing **3-ClO$_4$** with no added Bu_4NCl slowly became clear light blue overnight. After stirring was completed, the solvent was removed under reduced pressure. CH_2Cl_2 (5 mL) and HCl (5 mL, 1 M) were then added to the remaining residue and the mixture was stirred for one hour. Each mixture was transferred to a separatory funnel, and the organic layer was collected. The water layer was subsequently washed with additional aliquots of CH_2Cl_2, and the organic extracts were combined. The organic layer was washed again with aqueous HCl (5 mL, 1 M), followed by a wash with saturated brine solution. The organic layer was subsequently dried over sodium sulfate, filtered, and the filtrate brought to dryness. ^1H NMR data were collected and compared to known standards.

2.6. Treatment of the lithium salt of 2-chloro-1,3-diphenyl-1,3-propanedione with tetrabutylammonium benzoate

Lithium bis(trimethylsilyl) amide (0.012 mmol) was dissolved in Et_2O (~2 mL) and added to a vial containing 2-chloro-1,3-diphenyl-1,3-propanedione (0.012 mmol). The resulting mixture was stirred for about five minutes, during which time it became yellow in color. The solvent was removed under reduced pressure, and the residual solid was dissolved in CH_3CN (5 mL). This solution was added to solid tetrabutylammonium benzoate (0.012 mmol). The resulting mixture was stirred for 24 h at ambient temperature. Removal of the solvent under reduced pressure followed by a work-up identical to the reaction mixtures of **1-ClO$_4$** and **3-ClO$_4$** in the presence of added anion outlined above gave a solid product that was evaluated by ^{1}H NMR.

2.7. Synthesis of 2-(benzoyloxy)-1,3-diphenyl-1,3-propanedione

The following procedure was adapted from a previously reported synthesis [28]. 2-bromo-1,3-diphenyl-1,3-propanedione [29] (0.993 mmol) was dissolved in DMSO (30 mL). Addition of sodium benzoate (9.93 mmol) produced a yellow solution which was subsequently stirred for 30 min in air. Addition of H_2O (30 ml) resulted in the formation of a white precipitate. The mixed aqueous/organic solution was transferred to a separatory funnel and extracted with Et_2O (2 x 30 mL). The combined Et_2O extracts were then washed three times with an equal volume of water. The organic solution was then dried over Na_2SO_4, filtered, and the solvent was removed by rotary evaporation. The remaining crude, oily solid was dissolved in a minimal amount of hot methanol and placed in the freezer (−15 °C) overnight. A white solid that deposited was collected by filtration (156 mg, 46 %). mp 98–99 °C. ^{1}H NMR ($CDCl_3$) δ (ppm): 8.13 (d, J = 7.4 Hz, 4H), 8.08 (d, J = 7.2 Hz, 2H), 7.60 (m, 3H), 7.49 (t, J = 8.0 Hz, 3H), 7.45 (t, J = 7.8 Hz, 3H), 7.20 (s, 1H). ^{13}C{^{1}H} NMR ($CDCl_3$) δ (ppm): 191.1 (C═O), 165.0 (C═O), 134.4, 134.3, 133.8, 130.2, 129.64, 129.60, 128.8, 128.7, 80.8 (11 signals expected and observed). FTIR (KBr, cm^{-1}): 1725 ($\nu_{C=O}$), 1690 ($\nu_{C=O}$), 1590, 1400, 1270.

2.8. Synthesis and characterization of [(6-Ph$_2$TPA)Cu(PhC(O)C(OC(O)Ph)C(O)Ph)]ClO$_4$ (4)

Under an inert atmosphere at ~30 °C, $Cu(ClO_4)_2{\cdot}6H_2O$ (0.135 mmol) was dissolved in CH_3CN (~3 mL) and added to solid 6-Ph_2TPA (0.135 mmol). The resulting deep blue solution was stirred for 30 min. In a separate container, 2-(benzoyloxy)-1,3-diphenyl-1,3-propanedione (0.135 mmol) was combined with lithium bis(trimethylsilyl) amide (0.135 mmol) dissolved in Et_2O (~3 mL) and the resulting mixture was stirred for 5 min, forming a yellow-white murky solution. The two solutions were then combined and stirred for a minimum of 1 h to produce a green solution. The solvent was then removed under reduced pressure and the residual solid was dissolved in CH_2Cl_2. This solution was passed through a celite plug and the filtrate was brought to dryness under vacuum. Crystals suitable for X-ray diffraction were grown by vapor diffusion of Et_2O into a CH_2Cl_2 solution. The solid sample was recrystallized twice to ensure purity. (48 mg, 37 %). Anal. calc. for $C_{52}H_{41}ClCuN_4O_8{\cdot}0.1CH_2Cl_2$: C, 65.36; H, 4.34; N, 5.85. Found: C, 65.07; H, 4.40; N, 5.94. ESI-MS: m/z calc. for $C_{52}H_{41}CuN_4O_4$, 848.2 $[M-ClO_4]^+$; found 848.3 $[M-ClO_4]^+$. UV–vis (CH_3CN) λ_{max}, nm (ε, M^{-1} cm^{-1}): 361 (11004). FT-IR (KBr, cm^{-1}): 1740 ($\nu_{C=O}$), 1570, 1560, 1460, 1360, 1090 (ν_{ClO4}), 620 (ν_{ClO4}).

2.9. Synthesis and characterization of [(bpy)Cu(PhC(O)C(OC(O)Ph)C(O)Ph)]ClO$_4$ (5)

Under an inert atmosphere at ~30 °C, $Cu(ClO_4)_2{\cdot}6H_2O$ (0.135 mmol) was dissolved in CH_3CN (~3 mL) and added to solid 2,2′-bipyridine (bpy, 0.135 mmol). The resulting deep blue solution was stirred for 30 min. In a separate container, 2-(benzoyloxy)-1,3-diphenyl-1,3-propanedione (0.135 mmol) was combined with lithium bis(trimethylsilyl) amide (0.135 mmol) dissolved in Et_2O (~3 mL) and the resulting mixture was stirred for 5 min, forming a yellow-white murky solution. The two solutions were then combined and stirred for 1 h, becoming a green turbid solution. The solvent was then removed under reduced pressure. The remaining solid was dissolved in CH_3CN (~1 mL). Excess Et_2O was added to the solution which induced the precipitation of a green solid. The filtrate was decanted and the solid was washed with fresh Et_2O. The solid was dried under vacuum. Crystals of **5** suitable for X-ray diffraction were grown by diffusion of Et_2O into a CH_3CN solution containing a few drops of CH_2Cl_2. (28 mg, 31 %). Anal. calc. for $C_{32}H_{23}ClCuN_2O_8{\cdot}0.25CH_2Cl_2$: C, 56.91; H, 3.47; N, 4.12. Found: C, 56.65; H, 3.46; N, 4.10. ESI-MS: m/z calc. for $C_{32}H_{23}CuN_2O_4$, 562.1 $[M-ClO_4]^+$; found 562.2 $[M-ClO_4]^+$. UV–vis (CH_3CN) λ_{max}, nm (ε, M^{-1} cm^{-1}): 354 (14242). FT-IR (KBr, cm^{-1}): 1730($\nu_{C=O}$), 1560, 1460, 1340, 1110(ν_{ClO4}), 630(ν_{ClO4}).

2.10. X-ray crystallography

The structure of **4** was determined at the University of Montana. A crystal was mounted on a glass fiber using viscous oil and transferred to a Bruker D8 Venture using MoK_α radiation (λ = 0.71073 Å) for data collection at 100 K. Data were corrected for absorption using the SADABS [30] area detector absorption correction program. Using Olex2 [31], the structure was solved with the SHELXT [32] structure solution program using direct methods and refined with the SHELXL [32] refinement package using least squares minimization. All non-hydrogen atoms were refined with anisotropic thermal parameters. All hydrogen atoms were placed in geometrically calculated positions and refined using a riding model. Isotropic thermal parameters of the placed hydrogen atoms were fixed to 1.2 times the U value (1.5 times for methyl groups) of the atoms to which they are linked. The structure of **4** was found to contain severely disordered diethyl ether solvent molecules within voids in the lattice. Attempts at modeling this solvent were not able to produce a suitable model. The SQUEEZE [33] routine within PLATON [34] was used to account for the residual, diffuse electron density and the model was refined against these data. This analysis corrected for a total of 89 electrons per unit cell. This value is near the number required to account for two diethyl ether molecules (84 electrons). Calculations and refinements were carried out using APEX3 [35], SHELXTL [36], Olex2 [31], and PLATON [34].

The structure of **5** was determined at Utah State University. A single crystal was mounted on a glass fiber loop using viscous oil and transferred to a Rigaku XtaLAB Mini II Diffractometer using MoKα (λ = 0.71073 Å) radiation for data collection at 100 K. Data were corrected using a Gaussian grid (numerical integration), with a 0.5 mm 1D horizontal Gaussian beam correction for the graphite monochromator. Using Olex2 [31], the structure of **5** was solved using the SHELXT [32] structure solution program using direct methods and refined with the SHELXL [32] refinement package using least square minimization. All non-hydrogen atoms were refined with anisotropic thermal parameters. Hydrogen atoms were placed in geometrically calculated positions and refined using a riding model. Isotropic thermal parameters of all hydrogen atoms were fixed to 1.2 times the U value (1.5 times for methyl groups) of the atoms to which they are linked. Calculations and refinement of structures were carried out using CrysAlisPro [37], SHELXL [32], and Olex2 [31] software.

X-ray structural data (CIF) for **4** and **5** is available from the Cambridge Crystallographic Data Centre by email (deposit@ccdc.cam.ac.uk; CCDC 2310385 and 2311746).

2.11. EPR spectroscopy

Low temperature X-band EPR spectra of **4** and **5** were acquired on a Bruker EMX EPR spectrometer equipped with an OxfordITC503 liquid

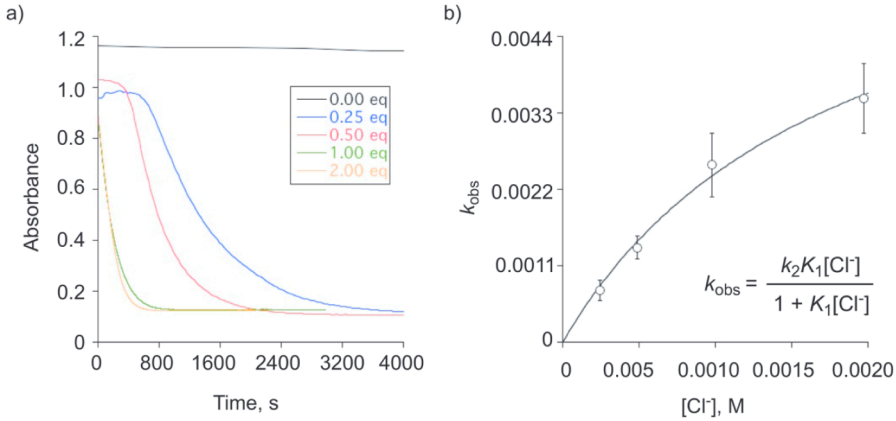

Fig. 1. a) Plot of absorbance (362 nm) versus time for the reaction of crystalline **1-ClO$_4$** (9.6 x 10^{-4} M) with O_2 in the absence and presence of varying amounts of chloride anion at 25 °C in dry CH_3CN. b) Plot of [Cl^-] versus the average k_{obs} for **1-ClO$_4$**. The saturation plot was fit to the equation shown.

Table 1
Length of the induction phase (in seconds) for the reactions of **1-ClO$_4$** and **3-ClO$_4$** with O_2 in the presence of varying amounts of added chloride anion at 25 °C.

Complex	0.00 eq Cl^-	0.25 eq Cl^-	0.50 eq Cl^-	1.00 eq Cl^-	2.00 eq Cl^-
1-ClO$_4$	NR	440	450	130	100
3-ClO$_4$	7700	330	50	50	0

helium cryostat. The spectra were collected at 12 K on samples that were ~0.5 mM in 1:1 acetonitrile/toluene. Other spectrometer settings: MW = 9.38 GHz (2 mW); time constant/conversion time = 21 ms; modulation amplitude 8 G (100 kHz); receiver gain = 20000; 10 scans.

2.12. DFT computations

All DFT computations were done with the use of Gaussian 16 ver. C.01 suite of programs [38]. The default implicit solvent model, i.e. integral equation formalism model IEFPCM [39], was employed with hardwired parameters for CH_3CN. B3LYP exchange–correlation functional was applied together with the D3 dispersion corrections with Becke-Johnson damping [40,41]. Two basis sets were used: def2-SVP for geometry optimization and frequency calculation and def2-TZVP for final electronic energy values [42]. The computational model included the cationic portion of the compound and the anion if it was directly coordinated to Cu(II). Models used to study the effect of water also included a single water molecule. The reported energy values are electronic energy computed with the def2-TZVP basis set with the IEFPCM solvent model included.

3. Results

3.1. Reexamination of the influence of chloride anion on the O_2-dependent C—C bond cleavage reaction of 1-ClO$_4$

We have previously published results of studies of the O_2-dependent C—C bond cleavage reactivity of **1-ClO$_4$** (Scheme 1) [21,22]. For this compound, kinetic experiments were performed in CH_3CN under pseudo first-order conditions with respect to O_2. A slow induction phase was followed by rapid first-order decay. Inclusion of a catalytic amount of chloride anion (from Bu_4NCl) was found to eliminate the induction phase through lowering of the barrier associated with O_2 activation

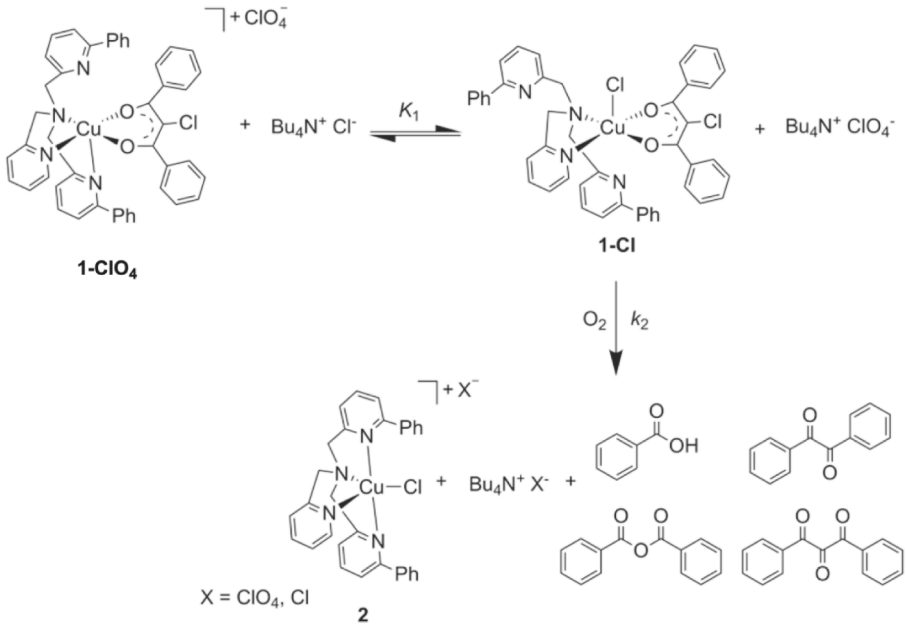

Scheme 3. Proposed equilibrium between **1-ClO$_4$** and **1-Cl** and subsequent irreversible O_2 activation step leading to O_2-dependent C—C bond cleavage.

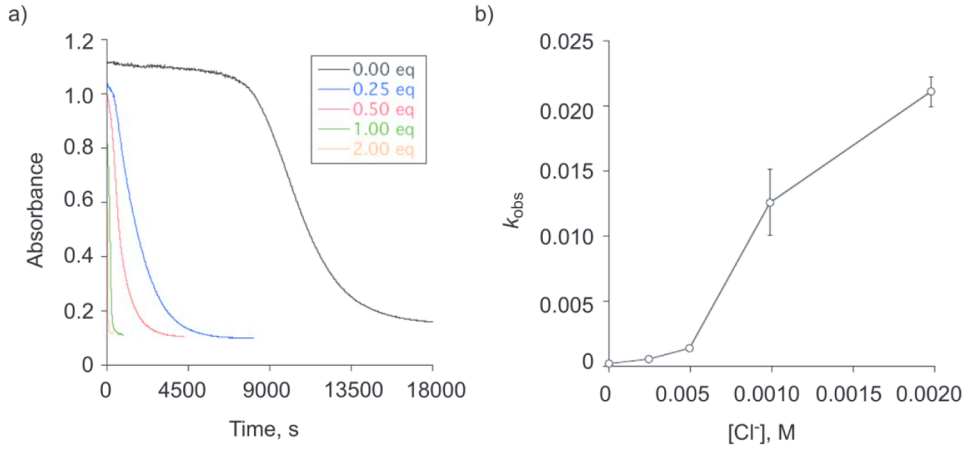

Fig. 2. a) Plot of absorbance (357 nm) versus time for the reaction of crystalline **3-ClO$_4$** (9.8 x 10^{-4} M) with O_2 in dry CH_3CN in the absence and presence of added amounts of chloride anion at 25 °C. b) Plot of [Cl^-] versus the average k_{obs} for **3-ClO$_4$**.

[22]. These prior studies of **1-ClO$_4$** involved use of complex that had been isolated via precipitation from CH_3CN:hexanes mixtures. For the updated studies reported herein, **1-ClO$_4$** was isolated via multiple re-crystallizations from Et_2O diffusion into CH_3CN solutions. When CH_3CN solutions prepared from isolated crystals of **1-ClO$_4$** were reexamined under the same pseudo first-order conditions with respect to O_2, no decay was observed up to 14 h at room temperature (Figs. 1(a) and S1). This result indicates that the precipitated samples must have contained trace chloride ion, which may have been generated via oxidative degradation or *retro*-Claisen type reactivity [23]. Consistent with prior results, when 0.25 equivalents of Bu_4NCl was added to a CH_3CN solution of crystalline **1-ClO$_4$**, reactivity with O_2 was observed (Fig. 1(a)) Increasing the amount of exogenous chloride added (up to two equivalents) resulted in complete loss of the induction phase (Table 1) and an increase in k_{obs} for the pseudo first-order decay portion (Fig. 1(a); Table S1). A plot of the rate of decay as a function of added chloride anion for **1-ClO$_4$** shows saturation behavior (Fig. 1(b)). The data were fit using a model for equilibrium binding of chloride anion to form **1-Cl,** followed by irreversible O_2 activation leading to C—C bond cleavage (Schemes 2(b) and 3). From the saturation curve fit, $K_1 \approx 550$ was determined. Based on prior work involving monitoring of *d-d* transitions of **1-ClO$_4$** as a function of the amount of added Cl^-, we proposed a similar equilibrium between **1-ClO$_4$** and **1-Cl** (Scheme 3), with $K_1 \approx 70$ [22]. Both approaches suggest weak coordination of chloride to the Cu (II) center in **1**. However, this coordination is important as the formation of **1-Cl** lowers the energy barrier for O_2 activation versus **1-ClO$_4$** [21,22]. Following O_2 activation, the reaction involves an irreversible O—O cleavage leading to a diphenylpropanetrione intermediate and eventually C—C cleavage products [22]. Evaluation of the products by ^{1}H NMR showed that reaction mixtures containing two equivalents of added chloride yielded the same organic products as previously reported (Scheme 3; Fig. S2) [21,22].

3.2. Chloride dependance of the O_2-dependent C—C bond cleavage reaction of 3-ClO$_4$

After reexamining the chloride dependence of **1-ClO$_4$** using crystalline sample, we also reinvestigated the O_2 reactivity of CH_3CN solutions of crystalline **3-ClO$_4$** [22] as a function of the amount of chloride ion added. Unlike **1-ClO$_4$**, after a long induction phase involving a slow decay, **3-ClO$_4$** undergoes reaction even in the absence of added chloride ion (Fig. 2(a)). Increasing the amount of added chloride anion reduces and then eliminates the induction phase and increases k_{obs}. Additional Cl^- up to two equivalents with respect to the concentration of the **3-ClO$_4$** produced an increase in k_{obs} suggesting that similar to **1-ClO$_4$** a chloride adduct may be forming that enables access to a lower energy O_2 activation pathway. It is important to note that the diketonate-derived organic products generated upon treatment of **3-ClO$_4$** with zero and two equivalents of added chloride anion (Figs. S3 and S4), respectively, are similar to those previously reported for **1-ClO$_4$** and prior studies of **3-ClO$_4$**. The products observed were benzoic acid, benzoic anhydride, benzil, diphenylpropanetrione, and 2,2-dihydroxy-propanedione (the hydrated form of diphenylpropanetrione).

Notably, the response of k_{obs} to increasing [Cl^-] for **3-ClO$_4$** does not

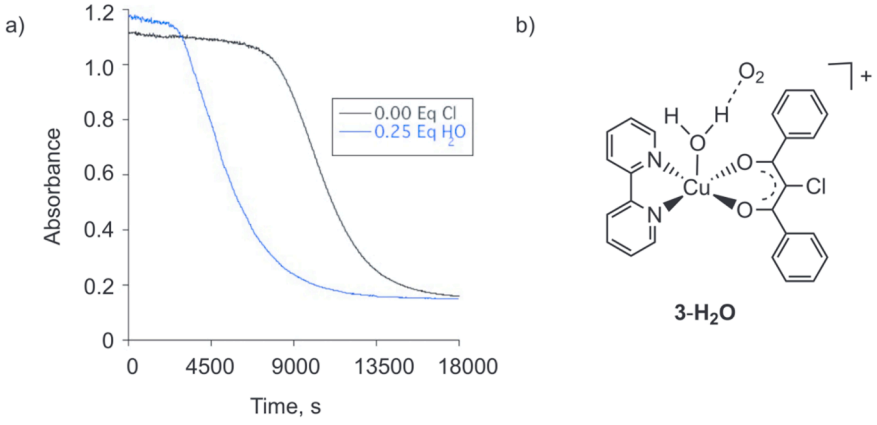

Fig. 3. a) Plot of absorbance vs time (monitored at 357 nm) for the reaction of crystalline **3-ClO$_4$** with O_2 in dry CH_3CN in the absence and presence of 0.25 eq of water at 25 °C. b) Drawing of a proposed water adduct **3-H$_2$O** that may facilitate the O_2 activation process.

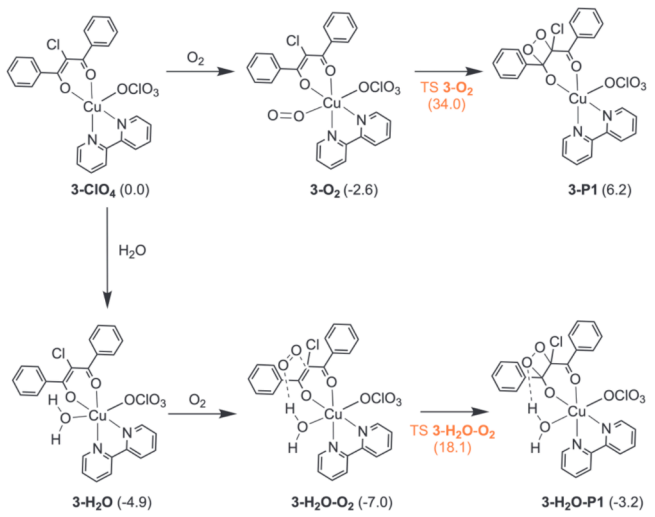

Scheme 4. O_2 activation pathways leading to peroxo formation.

exhibit saturation behavior akin to **1-ClO$_4$**. Instead, a substantial increase in k_{obs} is only evident upon the addition of >0.50 eq Cl^- (Fig. 2 (b)). This suggests that the effect of the added Bu_4NCl salt on the activation barrier is different than that found for **1-ClO$_4$**. Addition of more than two equivalents of chloride anion increases the rate further.

3.3. Evaluation of the effect of water in Bu_4NCl on the O_2 reactivity of 1-ClO$_4$ and 3-ClO$_4$

^{1}H NMR (Fig. S5) and IR analysis (Fig. S6) of the $[Bu_4N]Cl$ salt used to deliver chloride in the experiments outlined above provided evidence that ~0.5 eq of water is present per formula unit. With this being the case, we also examined the effect of added water on the O_2 reactivity of **1-ClO$_4$** and **3-ClO$_4$** in the absence of added chloride anion. While **1-ClO$_4$** shows no change in reactivity with added water, the induction phase for **3-ClO$_4$** is reduced in the presence of 0.25 eq of water (Fig. 3(a)). These preliminary studies suggested that the presence of water may facilitate lowering of the O_2 activation barrier possibly via structures such as **3-H$_2$O** (Fig. 3(b)).

3.4. Probing the effect of H_2O on the O_2 activation reactivity of 3-ClO$_4$ using computations

Density functional theory (DFT) calculations were performed to gain insight into the O_2 activation pathway and C—C cleavage in **3-ClO$_4$** and **3-H$_2$O** in the absence and presence of added chloride ion (**3-Cl** or **3-Cl-H$_2$O**) or coordinated solvent (**3-CH$_3$CN** and **3-H$_2$O-CH$_3$CN**). The DFT geometry optimized structures of these complexes are shown in Fig. S7. A detailed comparison of the bond distances involving the Cu(II) center in the X-ray structure of **3-ClO$_4$** versus the DFT geometry-optimized structure of this compound is given in Table S2. Overall, the bond distances and geometry (distorted square pyramidal; **3-ClO$_4$** (Xray): τ_5 =

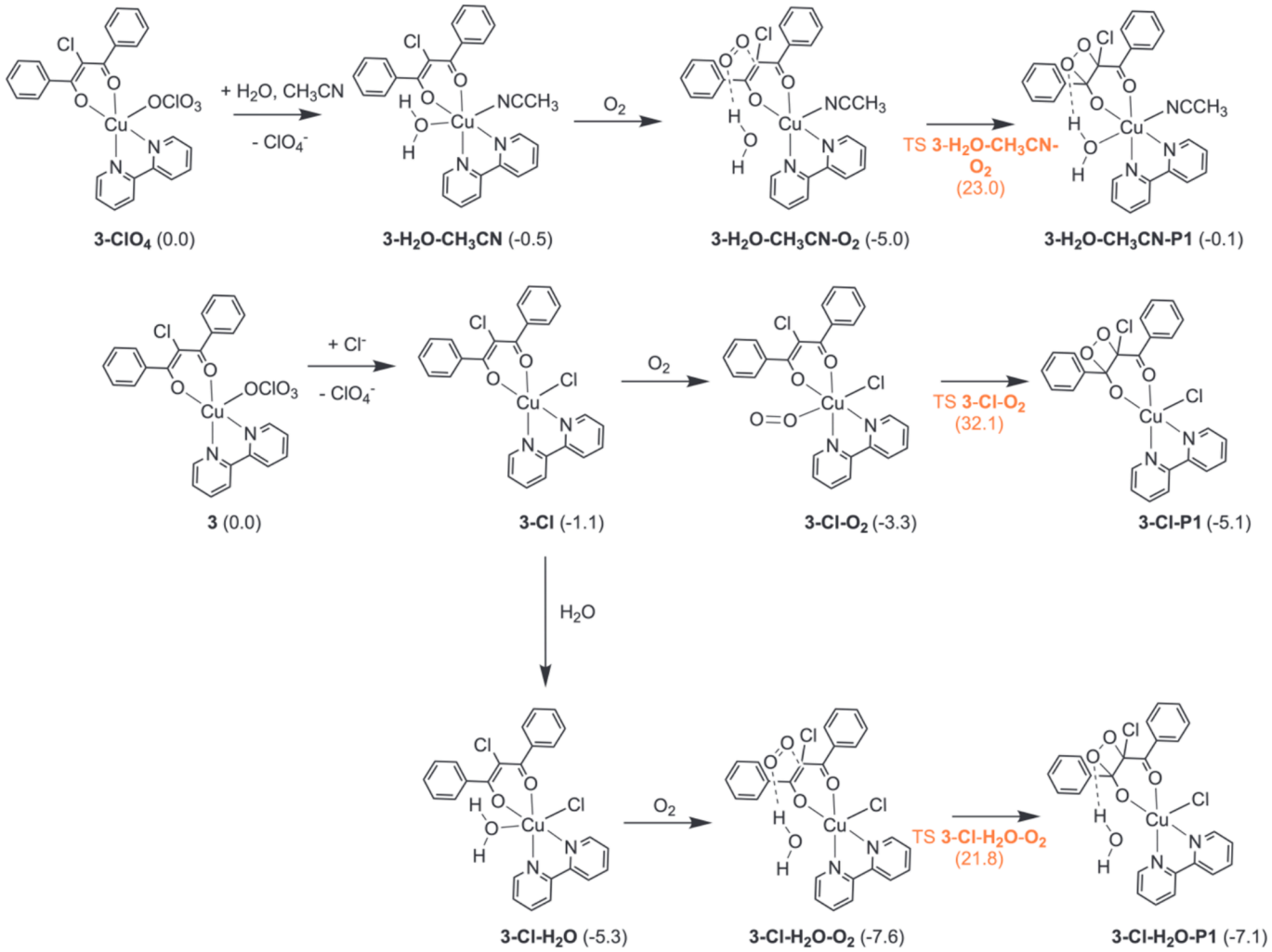

Scheme 5. Reaction pathways leading to peroxo formation wherein the axial perchlorate is replaced by solvent or chloride anion.

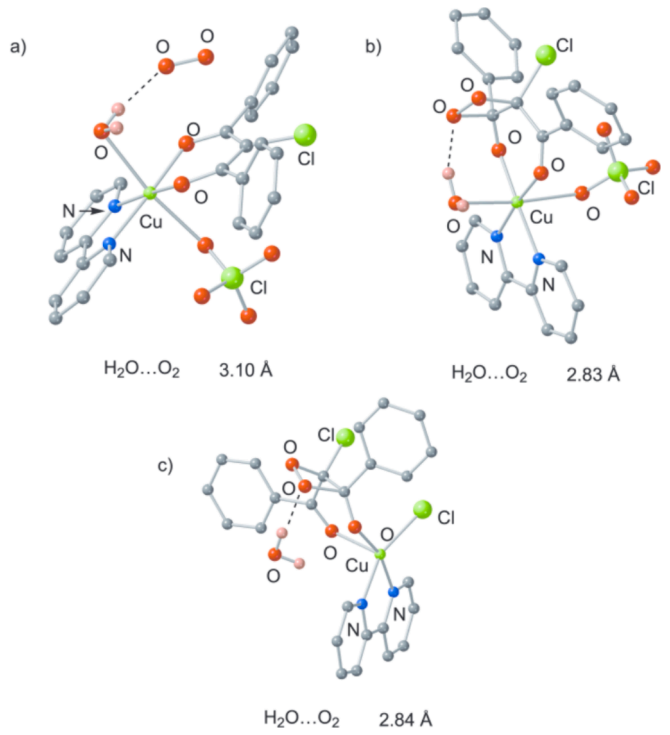

Fig. 4. DFT generated structures showing hydrogen bonding interactions between H_2O and O_2 in a) **3-H_2O-O_2**; b) **3-H_2O-O_2-P_1**; and c) **3-Cl-H_2O-P_1**.

0.027; **3-ClO_4** (DFT): 0.002)) [43] of the Cu(II) center in **3-ClO_4** determined by X-ray crystallography are well replicated by the DFT geometry-optimized structure, albeit with a ~0.1 Å longer Cu-$OClO_3$ interaction in the former.

The geometry optimized structure of **3-H_2O** contains a Cu(II) center that is distorted (elongated) octahedral. The Cu-OH_2 distance in geometry-optimized **3-H_2O** (2.426 Å) is slightly longer than that found for the axial positions in the $[Cu(H_2O)_6]^{2+}$ cation by X-ray crystallography and EXAFS [44]. Replacing the axial perchlorate anion in **3** with chloride (**3-Cl**) or solvent (**3-CH_3CN**) produces only slight changes in the bipyridine and diketonate Cu—O and Cu—N bond distances and geometry at the Cu(II) center (Fig. S7 and Table S2). Addition of water molecules in **3-Cl-H_2O** and **3-H_2O-CH_3CN** similarly produces little change in the chelate bonding interactions to the Cu(II) center. Notably, the coordinated water molecule in **3-Cl-H_2O** is only very weakly interacting (~2.7 Å) whereas the water molecule is more strongly interacting (~2.4 Å) in **3-H_2O** and **3-H_2O-CH_3CN.**

The rate determining step in the oxidative C—C bond cleavage reaction of **1-ClO_4** involves O_2 activation and formation of a peroxo species [22]. DFT methods used in that system provided evidence of a transition state energy for O_2 activation that was decreased by ~9 kcal upon axial chloride ligand binding to the Cu(II) center. In the current study, DFT methods have been used to examine the direct attack of O_2 on the central carbon of the enolate ligand leading to peroxo formation as a function of the ligands coordination to Cu(II) center. The calculations started from **3-ClO_4** having the coordinated perchlorate anion and examined how replacement of this axial ligand with solvent (CH_3CN) or chloride as shown in Schemes 4 and 5, and the addition of a sixth water ligand, affect the transition state energy for peroxo formation. The lowest energy pathways for peroxo formation from **3-ClO_4** are facilitated by the presence of a water ligand which can form a hydrogen bond with O_2 as it attacks the central carbon atom of the enolate and transforms into the peroxo group. Notably, the overall lowest transition state energy for peroxo formation, as computed with respect to the reactant state, was found for the perchlorate axial ligand (18.1 kcal/mol), similar values were computed for chloride (21.8 kcal/mol) and acetonitrile (23.0 kcal/mol) ligands. For each axial ligand, the addition of water lowers the activation barrier for peroxo formation by > 5.6 kcal/mol. Overall, for the conditions most relevant to experiment (involving addition of $Bu_4NCl{\cdot}0.5H_2O$), addition of both water and chloride is projected to lower the barrier for O_2 activation for **3-ClO_4** from ~34 to 22 kcal/mol.

Representations of the DFT generated **3-H_2O-O_2**, **3-H_2O-P1**, and **3-Cl-H_2O-P1** species are shown in Fig. 4. The hydrogen bonding interactions between water and O_2 facilitate both the approach of O_2 and stabilize the peroxo species with heteroatom distance of 2.8–3.1 Å. This occurs with the water molecule either coordinated (**3-H_2O-P1**) or released from (**3-Cl-H_2O-P1**) the Cu(II) center.

Following peroxo formation, rearrangement of the peroxo ligand to a bridging interaction with the Cu(II) center can lead to diphenylpropanetrione formation as previously described for **1-ClO_4** (Scheme 6) [22]. Alternatively, C—C cleavage directly from structures such as **3-Cl-H_2O-P1** can lead to carboxylic acid and α-ketoacid product formation. The product mixtures analyzed for **3-ClO_4** in the absence and presence of added chloride ion are consistent with a predominant diphenylpropanetrione pathway (Figs. S3 and S4).

3.5. *Effects of added benzoate anion on the O_2 reactivity of **1-ClO_4** and **3-ClO_4***

Benzoate/benzoic acid is produced in the O_2-dependent C—C cleavage reactions of **1-ClO_4** and **3-ClO_4**. Previously we reported that addition of tetrabutylammonium benzoate to **1-ClO_4** in CH_3CN likely results in coordination of the anion in the axial position similar to chloride (**1-OBz**, Fig. 5(a); log $K = 2.81(2)$) but unlike chloride does not reduce the induction phase or enhance the rate of the first-order decay process [22]. Notably, DFT studies had suggested that while benzoato coordination should lower the O_2 activation barrier similar to chloride, a subsequent step involving O—O and O-Cl cleavage is expected to provide a lower energy pathway in the chloride-containing system [22]. The difference in O_2 activation upon benzoate addition led us to reexamine the reactivity of both **1-ClO_4** and **3-ClO_4** with benzoate using various approaches.

As shown in Fig. 5(b), unlike chloride, which produces a rapid decay

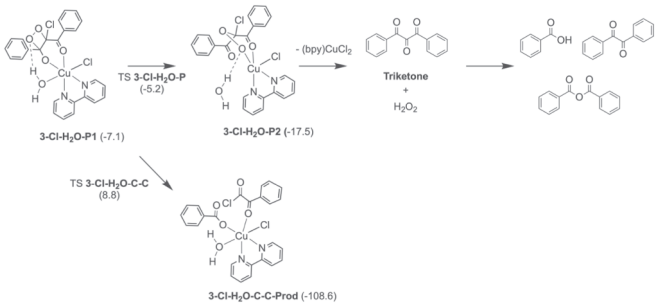

Scheme 6. Peroxo decomposition to products for **3-Cl-H_2O**.

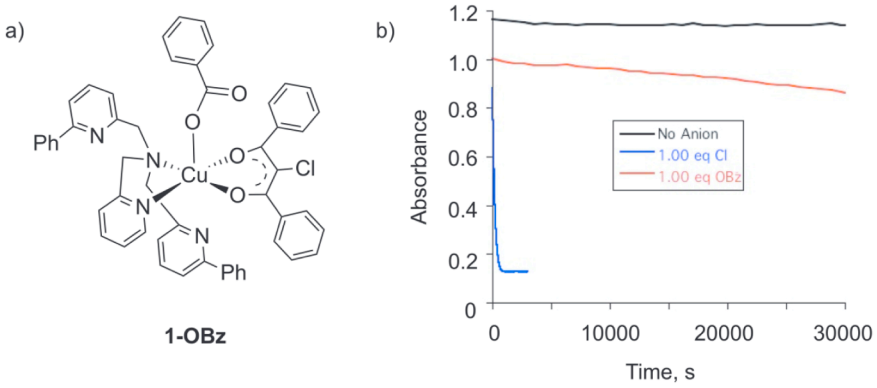

Fig. 5. a) Drawing of proposed benzoato adduct (**1-OBz**). b) Plot of absorbance (357 nm) versus time for the reaction of crystalline **1-ClO$_4$** with O_2 in dry CH_3CN in the absence and presence of one equivalent of tetrabutylammonium benzoate or chloride at 25 °C.

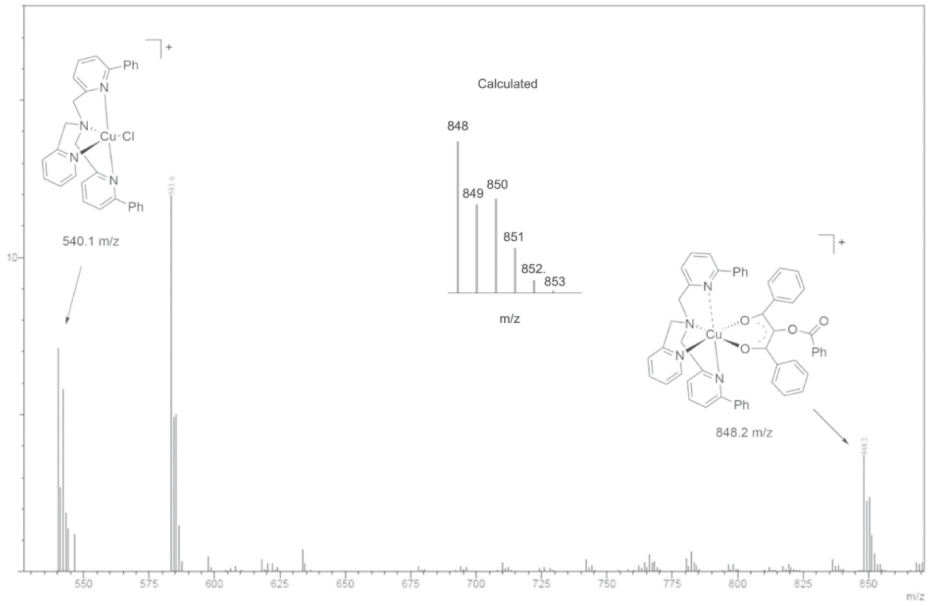

Fig. 6. ESI-MS spectrum of the reaction mixture of **1-ClO$_4$** with added tetrabutylammonium benzoate in CH_3CN after stirring for 16 h.

in the π → π* absorption band of **1-ClO$_4$** in the presence of O_2, the addition of benzoate anion at the same concentration produces only a very slow decay process. Notably, ESI-MS analysis of this reaction mixture revealed a new cluster at *m/z* 848.2 (Fig. 6), consistent with the monocation formulation [(6-Ph$_2$TPA)Cu(PhC(O)C(OC(O)-Ph)C(O)Ph)]$^+$ wherein the chloride substituent of the diketonate ligand has undergone substitution with benzoate. Identification of this cation indicates that the Cu(II) center facilitates the diketonate chloride exchange reactivity, as this reaction does not occur upon treatment of the neutral chlorodiketone with tetrabutylammonium benzoate in CH_3CN (Fig. S8). Based on spectroscopic data previously reported which suggests benzoato coordination to the Cu(II) center [22], we propose a reaction pathway as is outlined in Scheme 7. Organic recovery studies of a reaction mixture containing **1-ClO$_4$** and two equivalents of tetrabutylammonium benzoate stirred under air for 16 h yielded a product mixture comprised of unreacted chlorodiketone and 2-(benzoyloxy)-1,3-diphenyl-1,3-propanedione as major species and oxidative C—C bond cleavage products (benzil, benzoic anhydride) in lesser amounts (Fig. S9). As expected, performing the same reaction under N_2 yields only unreacted chlorodiketone and 2-(benzoyloxy)-1,3-diphenyl-1,3-propanedione (Fig. S10). We note that the benzoyloxy-substituted diketone was independently synthesized [28] and characterized (Figs. S11–S13) to confirm its formulation.

To gain insight into the potential oxidative C—C cleavage reactivity of **4**, the Cu(II) benzoyloxy diketonate complex was independently synthesized as outlined in Scheme S1. This complex was characterized by elemental analysis, X-ray crystallography, EPR, UV–Vis, ESI-MS and FT-IR (Figs. S14–S17). One of the two independent cations in the asymmetric unit of **4** is shown in Fig. 7. The Cu(II) center exhibits a six-coordinate geometry, with two weakly interacting phenyl-appended pyridyl donors (Cu1A-N3A: 2.458(3) Å; Cu1A-N4A: ~2.63 Å). The equatorial plane contains two Cu(II)-N bonds (1.986(3) Å; 2.066(3) Å) bonds, and the Cu—O bonds of the chelated diketonate moiety (Cu—O 1.920(2) and 1.929(2) Å, respectively). Overall, the structural features of **4** are very similar to those of the cationic portion of **1-ClO$_4$**, with the only difference being an additional axially interacting phenyl-appended pyridine donor (**1-ClO$_4$**: ~3.09; **4**: ~2.63 Å).

The ESI-MS of the **4** contains the expected pattern at [848.2 *m/z*]$^+$ (Fig. S14), which is identical to that found in the reaction mixture generated from addition of tetrabutylammonium benzoate to **1-ClO$_4$** in CH_3CN. The absorption spectrum of **4** contains a π-π* band at 361 nm (Fig. S15). The molar absorptivity for this band (~11,000 $M^{-1}cm^{-1}$) is

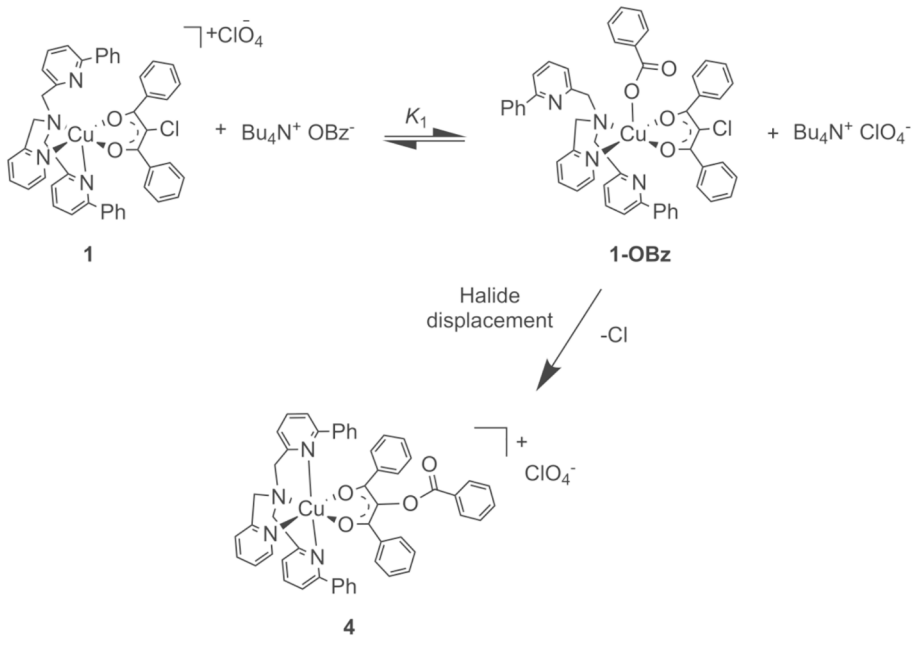

Scheme 7. Proposed benzoato coordination and diketonate substitution reactivity for **1**.

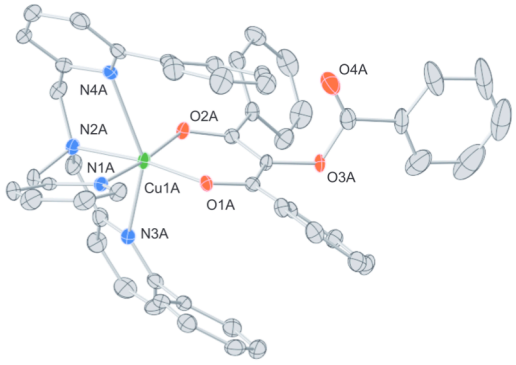

Fig. 7. Representation of one of the two independent cations in the asymmetric unit of **4**. Hydrogen atoms have been omitted for clarity. Ellipsoids are plotted at the 50% probability level.

similar to that of **1-ClO$_4$** (10,200 $M^{-1}cm^{-1}$). The solid-state IR spectrum of **4** contains a benzoyloxy carbonyl vibration at 1740 cm^{-1} (Fig. S16). An EPR spectrum collected as a frozen sample (1:1 CH_3CN:toluene at 12 K; Fig. S17) is consistent with an axial Cu(II) center, with $g_{||} \sim 2.26$, $g_{\perp} \sim 2.05$, and $A_{||} \sim 188$ Gauss.

The reactivity of **4** with O_2 was examined in the absence and presence of added chloride ion at 25(1) °C. After ~14 h, **4** exhibited no reaction (Fig. S17). This is like the results with **1-ClO$_4$**, where no reaction was observed in the absence of added chloride ion. In contrast, a reaction mixture containing **4** in the presence of one equivalent of tetrabutylammonium chloride showed a slow decay of the $\pi \rightarrow \pi^*$ diketonate absorption over the same period. Recovery of the organic products derived from the benzoyloxy diketone showed the presence of benzoic anhydride, benzil and unreacted 2-(benzoyloxy)-1,3-diphenyl-1,3-propanedione (Scheme 8; Fig. S18). These products indicate that the addition of chloride anion facilitates slow oxidative cleavage in the benzoyloxy-substituted derivative, albeit with significantly lower overall reactivity than the corresponding 2-chloro-1,3-diphenyl-1,3-propanedione.

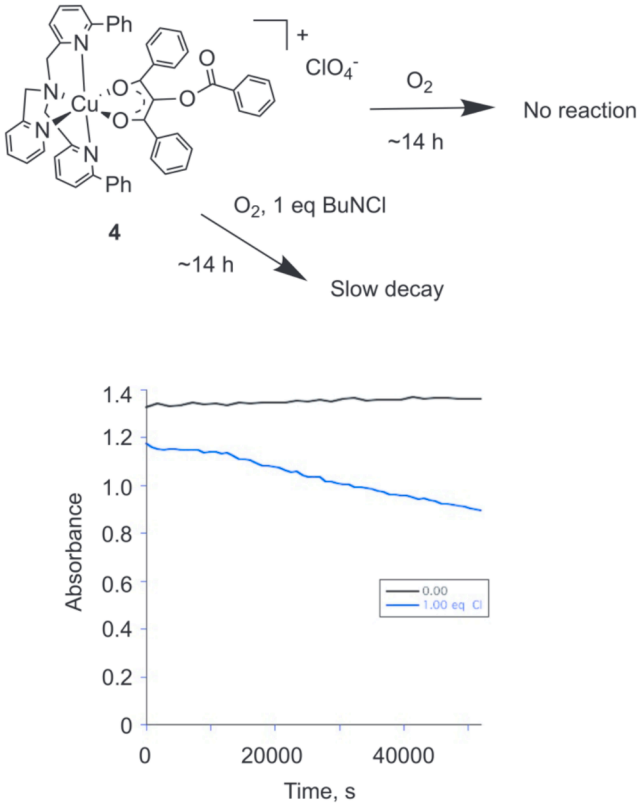

Scheme 8. Reactivity of 6-Ph$_2$TPA-ligated Cu(II) benzoyloxy diketonate complex **4** with O_2.

The reactivity of bpy-ligated **3-ClO$_4$** in the presence of benzoate anion under O_2 has not been previously examined. As shown in Fig. 8, treatment of **3-ClO$_4$** with tetrabutylammonium benzoate produced a slower decay relative to the same system containing added chloride. It should be noted that unlike the benzoate-containing reaction of **1-ClO$_4$**, the analogous reaction with **3-ClO$_4$** did go to completion after ~5000 s at 25(1) °C. Organic recovery experiments performed for the reaction of

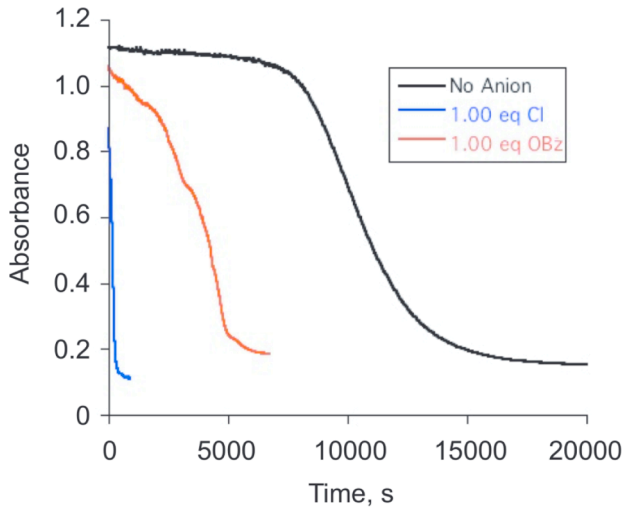

Fig. 8. Plot of absorbance (357 nm) vs time for the reaction of crystalline **3-ClO$_4$** with O_2 in dry CH_3CN in the absence and presence of 1.0 eq of tetrabutylammonium benzoate or chloride at 25(1) °C.

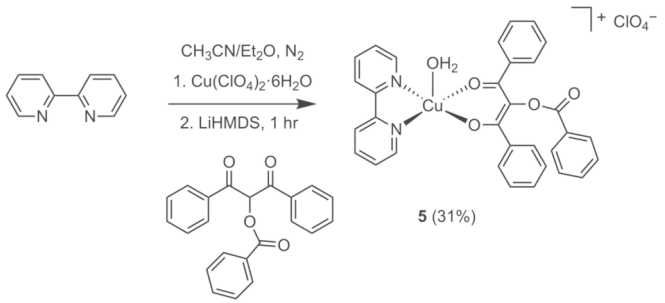

Scheme 9. Independent synthesis of **5**.

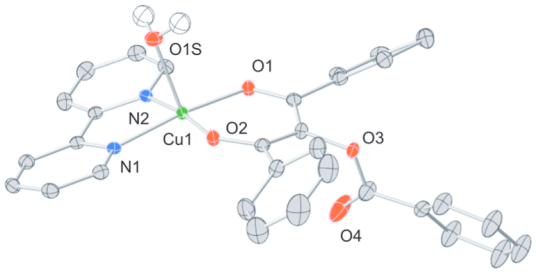

Fig. 9. A representation of the cationic portion of **5**. Hydrogen atoms have been omitted for clarity. Ellipsoids are plotted at the 50% probability level.

3-ClO$_4$ with O_2 in the presence of two equivalents of tetrabutylammonium benzoate revealed the formation of oxidative cleavage products – benzoic anhydride, benzoic acid, and a small amount of benzil, with no evidence for formation of the benzyloxy-substituted diketone (Fig. S19). We note that performing the same reaction under N_2 results in the formation of a significant amount benzoyloxy-substituted diketone (Fig. S20).

The decrease in the induction phase for the reaction of **3-ClO$_4$** with O_2 in the presence of benzoate anion may be due to the presence of water. As outlined above, water reduces the induction phase for the O_2 activation reaction of **3-ClO$_4$** in the absence of any added anions (*vida supra*). ^{1}H NMR and FTIR analysis (Figs. S21 and S22) indicate the presence of ~0.2 eq of H_2O per equivalent of the benzoate salt.

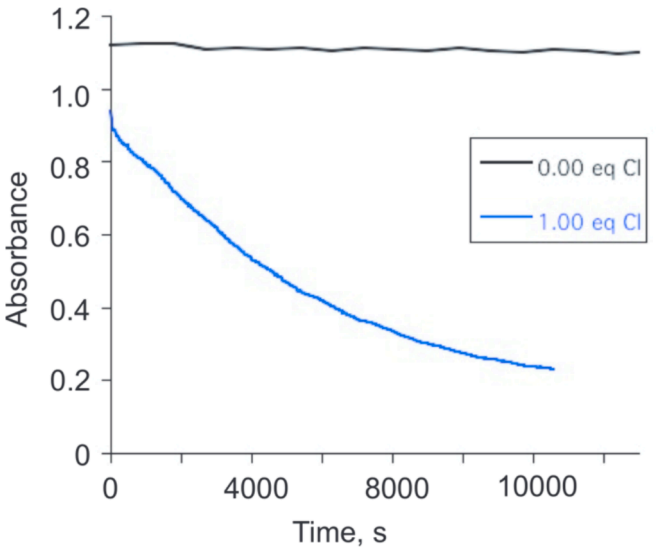

Fig. 10. Plot of absorbance (354 nm) vs time for the reaction of crystalline **5** with O_2 in dry CH_3CN in the absence and presence of one equivalent of tetrabutylammonium chloride at 25 °C.

For comparison to the chemistry of **4**, we independently synthesized and characterized the bpy-ligated Cu(II) benzoyloxy diketonate complex **5** (Scheme 9). The cationic portion of **5** is shown in Fig. 9. The Cu(II) exhibits a slightly distorted square pyramidal Cu(II) center ($\tau = 0.08$) [43] with similar Cu—N(1.9993(16) and 1.9888(16) Å) and Cu—O (1.9262(14) and 1.9260(14) Å) distances in the equatorial plane. Notably, a water molecule is coordinated to the Cu(II) center, with a Cu—O distance of 2.2637(15) Å. This ligand is relevant to the proposed water coordination that may impact O_2 activation in anion and solvent-coordinated forms of **3**.

In terms of spectroscopic properties, the solid-state IR spectrum of **5** contains a benzoyloxy carbonyl vibration at 1730 cm^{-1} (Fig. S23). The ESI-MS of **5** in CH_3CN displayed the expected cationic isotope cluster at *m/z* 562.2 (Fig. S24). The absorption spectrum of **5** contains a diketonate π-π* band at 354 nm (Fig. S25). EPR data for **5** collected on sample dissolved in 1:1 CH_3CN:toluene at 12 K indicated a highly axial Cu(II) center with $g_{||} \sim 2.25$, $g_{\perp} \sim 2.06$ and $A_{||} \sim 186$ Gauss (Fig. S26).

The reactivity of **5** with O_2 was examined in the absence and presence of added chloride anion at 25 °C. After ~14 h, **5** exhibited no reaction (Fig. 10). This is like the results with **4**, where no reaction was observed in the absence of added chloride ion. A reaction mixture containing one equivalent of **5** in the presence of two equivalents of tetrabutylammonium chloride showed a slow decay of the $\pi \rightarrow \pi^*$ diketonate absorption band over the same period. Ligand recovery from this reaction showed the presence of diketonate oxidative cleavage products, including benzoic acid, benzoic anhydride and benzil (Scheme 10; Fig. S27). This result demonstrates that chloride anion and/or the associated water within the salt can facilitate O_2 activation leading to C—C cleavage.

4. Discussion

4.1. Novel coordination chemistry contributions

Copper(II) salts are used extensively as catalysts in synthetic reactions employing O_2 as the terminal oxidant. A typical approach toward identifying the best catalyst for a particular oxidation is to screen

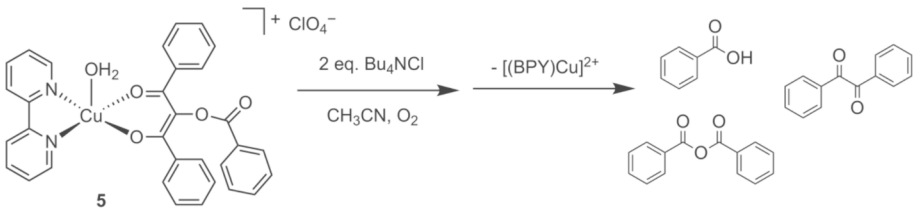

Scheme 10. Reaction of **5** with O_2 in the presence of two equivalents of Bu_4NCl.

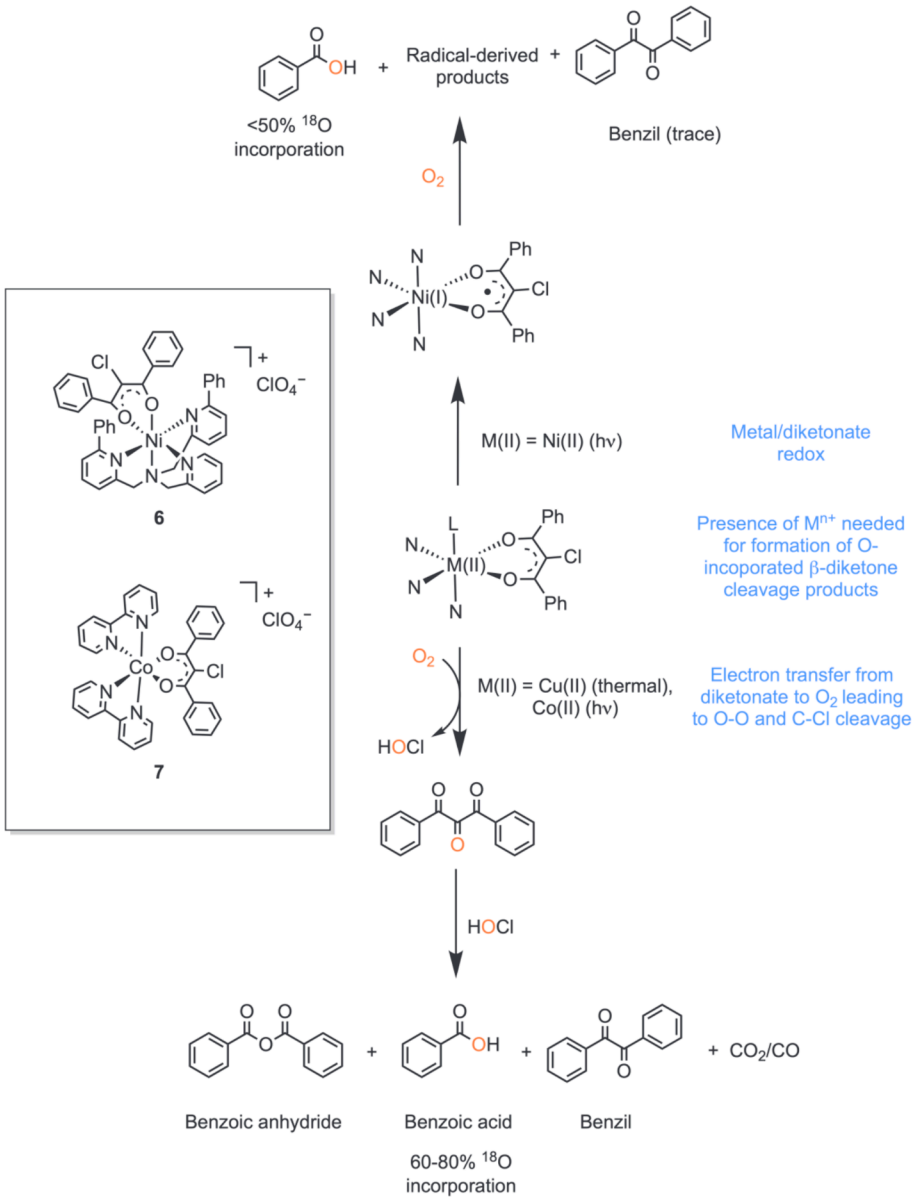

Scheme 11. Summary of reactions of divalent metal chlorodiketonate complexes with O_2.

the reaction using various Cu(I) and Cu(II) salts. For the most part, this type of approach focuses on optimizing product yield. To date, there have been few systematic studies to examine the effects on various anions on O_2 activation involving copper salts [5,15–17].

The chemistry outlined herein reveals the following primary findings:

(1) The bpy-ligated Cu(II) chlorodiketonate complex **3-ClO$_4$** is inherently more reactive with O_2 than 6-Ph$_2$TPA-ligated analog **1-ClO$_4$** at 25 °C. No added chloride is needed to facilitate O_2 reactivity for **3-ClO$_4$** but added water does enhance the rate of reactivity via hydrogen bonding interactions with O_2 and a subsequently formed peroxo species. Overall, these results show that the supporting chelate ligand and solvent provide important contributions in facilitating O_2 reactivity with the Cu(II) chlorodiketonate moiety.

(2) The bpy-ligated Cu(II) chlorodiketonate complex exhibits enhanced O_2 reactivity in the presence of water whereas no

similar effect was found for the 6-Ph_2TPA analog. We hypothesize that this is because a coordination position is readily available for H_2O binding in **3-ClO$_4$** whereas in **1-ClO$_4$** a H_2O ligand must compete with donors from the supporting 6-Ph_2TPA chelate ligand.

(3) The chloride substituent in the diketonate ligand of **1-ClO$_4$** and **3-ClO$_4$** will undergo displacement upon treatment of each complex with tetrabutylammonium benzoate. The Cu(II) benzoyloxy diketonate complexes **4** and **5** are formed, the formulations of which have been confirmed through independent synthesis and characterization.

(4) The Cu(II) benzoyloxy diketonate complexes **4** and **5** are unreactive with O_2 at 25 °C. Addition of chloride anion enhances the O_2 reactivity of **4** and **5**, however both are significantly less reactive in terms of producing oxidative C—C bond cleavage products than the chlorodiketonate analogs (**1-ClO$_4$** and **3-ClO$_4$**).

Mononuclear Cu(II) dibenzoylmethane complexes supported by a 2,2′-bipyridine or phenanthroline ligand are relatively rare [45–50], with our laboratory reporting the only O_2 reactive complexes (**1-ClO$_4$** and **3-ClO$_4$**) to date. The formation of the α-benzoyloxydiketonate complexes (**4** and **5**) via substitution of the diketonate chloro substituent in **1-ClO$_4$** and **3-ClO$_4$** is facilitated by the presence of the Cu(II) center. To our knowledge, these are the first transition metal complexes having an α-benzoyloxydiketonate ligands. Typically, α-acyloxydiketones are formed via reactions involving the unsubstituted diketone, hypervalent iodine reagents and a halide source [46,51–55]. The observed slow O_2 reactivity of **4** and **5** relative to **1-ClO$_4$** and **3-ClO$_4$** in the presence of added chloride anion to provide oxidative cleavage products indicates that the nature of the diketonate substituent can be used to tune O_2 reactivity in these novel Cu(II) complexes.

4.2 O_2-dependent C—C cleavage and diketones

Studies of the O_2-dependent reactivity of divalent metal chlorodiketonate complexes such as those described herein contribute to understanding fundamental mechanistic issues related to O_2 activation and C—C bond cleavage product formation. Such investigations are relevant toward gaining insight relevant to the reaction catalyzed by diketone dioxygenase (Dke1) [20] and synthetically useful M(II)/O_2-mediated diketone cleavage reactions [5]. To date, very few synthetic first row metal complexes have been reported that exhibit O_2-dependent β-diketone oxidative cleavage [56–61]. It is notable that divalent metal chlorodiketonate complexes show differences in reactivity with O_2 depending on the nature of the metal ion (Scheme 11). A coordinatively saturated Ni(II) chlorodiketonate complex (**6**, Scheme 11) requires UV-light to initiate O_2 reactivity [62]. In this case, the product distribution suggests a reaction pathway that involves a Ni(I)-chlorodiketonate radical species which subsequently reacts with O_2 to give C—C cleavage products (benzoic acid). The Cu(II) systems outlined herein are thermally reactive with O_2, with reaction occurring spontaneously or upon the introduction of chloride anion [21,22]. Nitrogen donor ligand-supported Co(II) chlorodiketonate complexes such as **7** (Scheme 11) require illumination to undergo reaction with O_2 [63]. The product distributions and ^{18}O incorporation in the Co(II) complex-derived products are like those identified for the Cu(II) chlorodiketonate derivative **1-ClO$_4$**. Both systems facilitate O—O and C—Cl bond cleavage primarily leading to diphenylpropanetrione formation from which C—C cleavage proceeds likely via reaction with HOCl generated in the reaction mixture. Overall, it is evident that the ligand composition within the primary coordination sphere and the nature of the divalent metal ion impact the pathway leading to O_2 activation and C—C cleavage in these systems. For the chlorodiketonate substrates studied herein, it is important to remember that in the absence of a metal ion, no oxygen incorporated products are generated [64].

CRediT authorship contribution statement

Josiah G.D. Elsberg: Writing – original draft, Visualization, Methodology, Investigation. **Tomasz Borowski:** Writing – original draft, Visualization, Methodology, Investigation. **Eric W. Reinheimer:** Methodology. **Lisa M. Berreau:** Writing – original draft, Supervision, Project administration, Funding acquisition, Formal analysis, Conceptualization.

Declaration of competing interest

The authors declare that they have no known competing financial interests or personal relationships that could have appeared to influence the work reported in this paper.

Data availability

Data will be made available upon request. Computational structures are available at 10.19061/iochem-bd-4-70.

Acknowledgments

The authors thank the National Science Foundation for support of this work (CHE-1664977) and for funding in support of the acquisition of NMR and X-ray crystallography instruments (CHE-1429195; CHE-1828764) used for data collection in this work. We gratefully acknowledge Polish high-performance computing infrastructure PLGrid (HPC Centers: ACK Cyfronet AGH) for providing computer facilities and support within computational grant no. PLG/2023/016769. X-ray crystallographic studies of 4 were performed at the University of Montana (NIH, COBRE NIGMS P30GM140963).

Appendix A. Supplementary data

Supplementary data to this article can be found online at https://doi.org/10.1016/j.ica.2024.122203.

References

[1] R. Trammell, K. Rajabimoghadam, I. Garcia-Bosch, Chem. Rev. 119 (2019) 2954–3031.
[2] H. Liu, M. Wang, H. Li, N. Luo, S. Xu, F. Weng, J. Catal. 346 (2017) 170–179.
[3] Y.F. Liang, N. Jiao, Acc. Chem. Res. 50 (2017) 1640–1653.
[4] C. Tang, X. Qiu, Z. Cheng, N. Jiao, Chem. Soc. Rev. 50 (2021) 8067–8101.
[5] C. Zhang, P. Feng, N. Jiao, J. Am. Chem. Soc. 135 (2013) 15257–15262.
[6] J. Zhang, C. Liu, M. Yang, Z. Fang, K. Guo, Tetrahedron Lett. 61 (2020) 152555.
[7] Y. Yu, Y. Zhang, C. Sun, L. Shi, W. Wang, H. Li, J. Org. Chem. 85 (2020) 2725–2732.
[8] C. Xu, Y. Wang, L. Bai, J. Org. Chem. 85 (2020) 12579–12584.
[9] M. Brendel, P.R. Sakhare, G. Dahiya, P. Subramanian, K.P. Kaliappan, J. Org. Chem. 85 (2020) 8102–8110.
[10] N. Vodnala, R. Gujjarappa, C.K. Hazra, D. Kaldhi, A.K. Kabi, U. Beifuss, C. C. Malakar, Adv. Synth. Catal. 361 (2019) 135–145.
[11] L. Deng, B. Huang, Y. Liu, Org. Biomol. Chem. 16 (2018) 1552–1556.
[12] C. Liu, Z. Yang, Y. Zeng, Z. Fang, K. Guo, Org. Chem. Front. 4 (2017) 2375–2379.
[13] X. Chen, Y. Peng, Y. Li, M. Wu, H. Guo, J. Wang, S. Sun, RSC Adv. 7 (2017) 18588–18591.
[14] W.B. Cao, X.Q. Chu, Y. Zhou, L. Yin, X.P. Xu, S.J. Ji, Chem. Commun. 53 (2017) 6601–6604.
[15] K. Fagnou, M.Lautens, Angew. Chem. Int. Ed. 41 (2002) 26–47.
[16] H. Yi, Z. Liao, G. Zhang, G. Zhang, C. Fan, X. Zhang, E.E. Bunel, C.W. Pao, J.F. Lee, A. Lei, Chem. Eur. J. 21 (2015) 18925–18929.
[17] Y. Deng, G. Zhang, X. Qi, C. Liu, J.T. Miller, A.J. Kropf, E.E. Bunel, Y. Lan, A. Lei, Chem. Commun. 51 (2015) 318–321.
[18] P.J. Sarver, V. Bacauanu, D.M. Schultz, D.A. DiRocco, Y.-H. Lam, E.C. Sherer, D.W. C. MacMillan, Nat. Chem. 12 (2020) 459–467.
[19] D.E. Diaz, D.A. Quist, A.E. Herzog, A.W. Schaefer, I. Kipouros, M. Bhadra, E. I. Solomon, K.D. Karlin, Angew. Chem. Int. Ed. Engl. 58 (2019) 17572–17576.
[20] G.D. Straganz, B. Nidetzky, J. Am. Chem. Soc. 127 (2005) 12306–12314.
[21] C.J. Allpress, A. Milaczewska, T. Borowski, J.R. Bennett, D.L. Tierney, A.M. Arif, L. M. Berreau, J. Am. Chem. Soc. 136 (2014) 7821–7824.
[22] S.L. Saraf, A. Milaczewska, T. Borowski, C.D. James, D.L. Tierney, M. Popova, A. M. Arif, L.M. Berreau, Inorg. Chem. 55 (2016) 6916–6928.

[23] J.G.D. Elsberg, S.N. Anderson, D.L. Tierney, E.W. Reinheimer, L.M. Berreau, Dalton Trans. 50 (2021) 1712–1720.
[24] D.B.G. Williams, M. Lawton, J. Org. Chem. 75 (2010) 8351–8354.
[25] M.M. Makowska-Grzyska, E. Szajna, C.E. Shipley, A.M. Arif, M.H. Mitchell, J. A. Halfen, L.M. Berreau, Inorg. Chem. 42 (2003) 7472–7488.
[26] Z.S. Zhou, L. Li, X.H. He, Chin. Chem. Lett. 23 (2012) 1213–1216.
[27] W.C. Wolsey, J. Chem Ed. 50 (1973) 335–337.
[28] D. Barillier, P. Riolt, J. Vialle, Bull. Chem. Fr. 3–4 (1976) 444–448.
[29] A. Giovannitti, S.M. Seifermann, A. Bihlmeier, T. Muller, F. Topic, K. Rissanen, M. Nieger, W. Klopper, S. Bräse, Eur. J. Org. Chem. (2013) 7907–7913.
[30] G.M. Sheldrick, University of Göttinggen, Germany, 1996.
[31] O.V. Dolomanov, L.J. Bourhis, R.J. Gildea, J.A.K. Howard, H. Puschmann, J. Appl. Cryst. 42 (2009) 339–341.
[32] G.M. Sheldrick, Acta Crystallogr. A 71 (2015) 3–8.
[33] A.L. Spek, Acta Crystallogr. C 71 (2015) 9–18.
[34] A.L. Spek, Acta Crystallogr. D Biol. Crystallogr. 65 (Pt 2) (2009) 148–155.
[35] Bruker, APEX3, Bruker AXS Inc., Madison, Wisconsin, USA. 2016.
[36] G.M. Sheldrick, Acta Crystallogr. A (2008) 64.
[37] CrysAlisPro 171 (40) (2019) 45a.
[38] M.J. Frisch, G.W. Trucks, H.B. Schlegel, G.E. Scuseria, M.A. Robb, J.R. Cheeseman, G. Scalmani, V. Barone, G.A. Petersson, H. Nakatsuji, X. Li, M. Caricato, A. V. Marenich, J. Bloino, B.G. Janesko, R. Gomperts, B. Mennucci, H.P. Hratchian, J. V. Ortiz, A.F. Izmaylov, J.L. Sonnenberg, D. Williams-Young, F. Ding, F. Lipparini, F. Egidi, J. Goings, B. Peng, A. Petrone, T. Henderson, D. Ranasinghe, V. G. Zakrzewski, J. Gao, N. Rega, G. Zheng, W. Liang, M. Hada, M. Ehara, K. Toyota, R. Fukuda, J. Hasegawa, M. Ishida, T. Nakajima, Y. Honda, O. Kitao, H. Nakai, T. Vreven, K. Throssell, J.A. Montgomery Jr., J.E. Peralta, F. Ogliaro, M. J. Bearpark, J.J. Heyd, E.N. Brothers, K.N. Kudin, V.N. Staroverov, T.A. Keith, R. Kobayashi, J. Normand, K. Raghavachari, A.P. Rendell, J.C. Burant, S.S. Iyengar, J. Tomasi, M. Cossi, J.M. Millam, M. Klene, C. Adamo, R. Cammi, J.W. Ochterski, R.L. Martin, K. Morokuma, O. Farkas, J.B. Foresman, D.J. Fox, Gaussian 16, Revision C.01, Gaussian Inc, Wallingford CT, 2016.
[39] G. Scalmani, M.J. Frisch, J. Chem. Phys. 132 (2010) 114110.
[40] A.D. Becke, J. Chem. Phys. 98 (1993) 5648–5652.
[41] S. Grimme, S. Ehrlich, L. Goerigk, J. Comp. Chem. 32 (2011) 1456–1465.
[42] S. Grimme, J. Antony, S. Ehrlich, H. Kreig, J. Chem. Phys. 132 (2010) 154104.
[43] A.W. Addison, N.T. Rao, J. Reedijk, J. van Rijn, G.C. Verschoor, J. Chem. Soc. Dalton Trans. (1984) 1349–1356.
[44] I. Persson, D. Lundberg, E.G. Bajnoczi, K. Klementiev, J. Just, K.G.V. Sigfridsson Clauss, Inorg. Chem. 59 (2020) 9538–9550.
[45] Y. Yamane, M. Miyazaki, S. Ikeda, N. Yamaji, Chem. Pharm. Bull. 18 (1970) 1589–1594.
[46] K.M. Purohit, D.V.R. Rao, Indian J. Chem. A 21A (1982) 437–439.
[47] G.N. Rao, J.S. Thakur, Indian J. Chem. 12 (1974) 861–864.
[48] M. Munakata, M. Harada, S. Niina, Inorg. Chem. 15 (1976) 1727–1729.
[49] K. Gopalakrishnan, U. Chudasama, P.K. Bhattacharya, J. Indian Chem. Soc. 56 (1979) 445–447.
[50] H. Oluwatola Omoregie, N. Obi-Egbedi, J. Woods, Int. J. Chem. 6 (2014) 71–82.
[51] B. Podolesov, J. Org. Chem. 49 (1984) 2644–2646.
[52] M. Miyamoto, M.M. Hoque, Y. Senoh, M.I. Ali, H. Nemeto, T. Mandal, Eur. J. Org. Chem. (2018) 2841–2845.
[53] W.-B. Liu, C. Chen, Q. Zhang, Z.-B. Zhu, Beilstein J. Org. Chem. 7 (2011) 1436–1440.
[54] M. Moriarity, O. Prakash, Org. React. 54 (2004) 273–418.
[55] M. Fujio, A. Moriyasu, T. Tatsuo, I. Juichi, Bull. Chem. Soc. Jpn 51 (1978) 335–336.
[56] I. Siewert, C. Limberg, S. Demeshko, E. Hoppe, Chem. Eur. J. 14 (2008) 9377–9388.
[57] I. Siewert, C. Limberg, Angew. Chem. Int. Ed. 47 (2008) 7953–7956.
[58] H. Park, M.M. Bittner, J.S. Baus, S.V. Lindeman, A.T. Fiedler, Inorg. Chem. 51 (2012) 10279–10289.
[59] K. Schroder, B. Join, A.J. Amali, K. Junge, X. Ribas, M. Costas, M. Beller, Angew. Chem. Int. Ed. Engl. 50 (2011) 1425–1429.
[60] S. Hoof, M. Sallmann, M. Herwig, B. Braun-Cula, C. Limberg, Dalton Trans. 46 (2017) 16792–16795.
[61] C. Yang, D. Liu, T. Wang, F. Sun, S. Qui, G. Wu, Chem. Commun. 57 (2021) 9462–9465.
[62] C.J. Allpress, A.M. Arif, D.T. Houghton, L.M. Berreau, Chem. Eur. J. 17 (2011) 14962–14973.
[63] S.N. Anderson, J.G.D. Elsberg, L.M. Berreau, Dalton Trans. 52 (2023) 4152–4160.
[64] B. Košmrlj, B. Sket, Org. Lett. 9 (2007) 3993–3996.